A study of the effect of flow pulsations on the flow distribution within ceramic contoured catalyst substrates

Benjamin, S.F. , Roberts, C.A. and Wollin, J.

SAE TECHNICAL PAPER SERIES

2001-01-1996

A Study of the Effect of Flow Pulsations on the Flow Distribution within Ceramic Contoured Catalyst Substrates

S. F. Benjamin, C. A. Roberts and J. Wollin
Coventry Univ.

Reprinted From: General Emissions Research and Development (SP–1631)

The Engineering Society For Advancing Mobility Land Sea Air and Space®
INTERNATIONAL

International Spring Fuels & Lubricants Meeting & Exhibition
Orlando, Florida
May 7-9, 2001

400 Commonwealth Drive, Warrendale, PA 15096-0001 U.S.A. Tel: (724) 776-4841 Fax: (724) 776-5760

ISSN 0148-7191

Printed in USA

2001-01-1996

A Study of the Effect of Flow Pulsations on the Flow Distribution within Ceramic Contoured Catalyst Substrates

S. F. Benjamin, C. A. Roberts and J. Wollin
Coventry Univ.

ABSTRACT

This study examines the effect of pulsating flow on the flow distribution through contoured substrates. Three ceramic contoured substrates of equal volume were assessed. Two of the substrates were cone shaped with different cone angles and one had a dome shaped front face. The flow distribution was measured for a range of flow rates and pulsation frequencies. Computational Fluid Dynamics (CFD) simulations were also performed. It is shown how a contoured substrate can provide improvements in flow uniformity and that they are less sensitive to changes in flow rate and pulsation frequency when compared to the case of a standard substrate. Improvements in the prediction of flow distribution are reported when substrate “entrance effects” are accounted for.

INTRODUCTION

Maldistributed flow due to separation caused by wide-angle diffusers is often encountered in standard automotive exhaust catalyst systems. This can have an adverse affect on conversion efficiency, catalyst durability and pressure loss [1, 2]. One possible method of improving the flow distribution is by shaping the substrate. This was shown by Wollin *et al*. in a previous report [3]. An example of a shaped substrate can be seen in figure 1. The previous study was undertaken using steady flow, however pulsating flow is clearly of interest in exhaust systems.

Several steady flow studies were reported in the previous study [3] such as Heibel *et al.* [4], Schönfelder [5] and Holmgren *et al.* [6].

Two further investigations have since been published on the steady flow performance of shaped substrates. Shuai *et al.* [7, 8] confirmed the beneficial effects that can be obtained by shaped substrates.

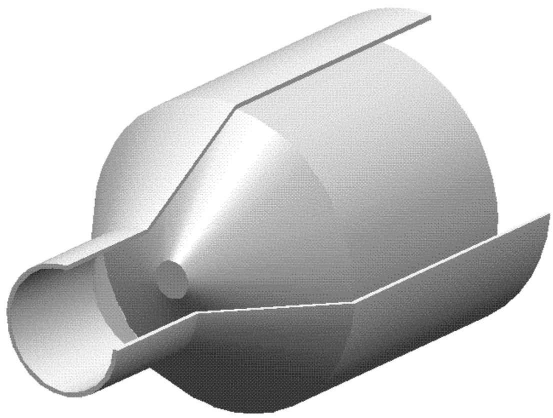

Figure 1 Contura substrate with diffuser

The objective of this study was to investigate the effect of pulsating flow on shaped substrates. To achieve this four different substrates have been studied at different flow rates and pulsation frequencies. A standard substrate, for reference is compared to two cone shaped substrates according to the Corning Contura concept and to one dome shaped substrate according to the Coventry University AeroCat concept.

EXPERIMENTAL METHOD

SUBSTRATE DESCRIPTION - All substrates were unwashcoated and taken from the same batch to minimise manufacturing variance. The volumes of the substrates were as close as the manufacturing process allowed (~1.11 dm^3). The substrates were of circular section of diameter 118 mm and cell density of approximately 390 cells per square inch (cpsi). A microscope was used to measure the cell width and wall thickness, which were found to be approximately 1.08 and 0.161 mm respectively. The dimensions of the substrates as received are given in table 1.

measures in mm	Contura 1	Contura 2	AeroCat	Standard
Total length	122.8	126.6	114.4	102.2
Length shaped part	33.6	40.0	27.0	N/A
Length cylindrical part	89.2	86.6	87.4	N/A
Tip diameter	14.7	14.7	N/A	N/A
Front angle (degrees)	33.0	37.8	N/A	N/A

Table 1 Summary of external dimensions

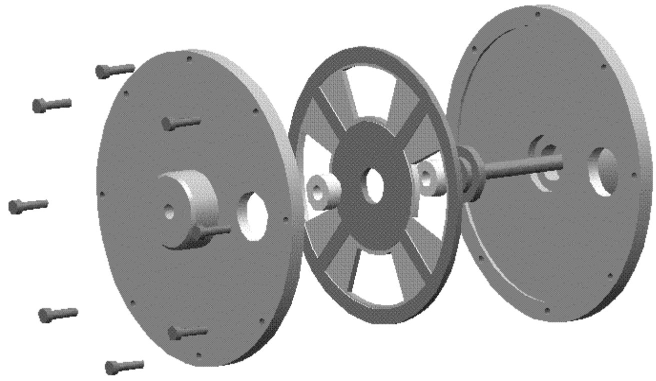

Figure 3 Exploded schematic of pulse generator

TEST RIG - A schematic layout of the iso-thermal test rig used in this study can be seen in figure 2. The test rig was supplied with compressed air from two receivers via a main valve (1). A pressure gauge (2) monitors the supply pressure, which was reduced from ~100 psi to ~20 psi by a valve (3). A second pressure gauge monitors the up-stream rig pressure (4). A filter (5) was used to avoid oil contamination. The mass flow rate was controlled by an adjustment valve (6). A safety relief valve rated at 80 psi was used to avoid damage to the rig (7). Rig pressure was monitored by a pressure gauge (8). Flow rate was measured using a viscous flow meter (VFM) (10). Up-stream of the VFM was a 50 mm flow straightener (9) used to ensure a smooth inlet to the VFM. The viscous flow meter was connected to a digital manometer FCO16 from Furness Controls. A plenum incorporating a flow straightner (11) was used to avoid swirl components in the flow and a contracting nozzle (12) produced a uniform velocity profile at the diffuser inlet under steady flow conditions. The pulsations were achieved using a pulse generator (13) of which a schematic can be seen in figure 3. A tube (14) was used to hold flow straighteners to achieve uniform flow as described below. A 60 degree (15) total angle axially symmetric diffuser was used in the experiments. The length of the diffuser was 61.5 mm and it featured a 20 mm inlet section prior to the diffuser throat. The inlet pipe diameter, on which all Reynolds numbers were based, was 48 mm. On the test substrate (16) an outlet sleeve (17) was used to avoid entrainment of surrounding air.

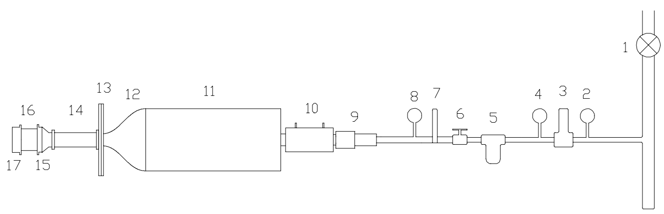

Figure 2 Schematic of iso-thermal flow rig

Figure 4 shows a typical inlet velocity pulse. As can be seen the pulse shape was approximately sinusoidal with velocity amplitude approximately equal to the mean.

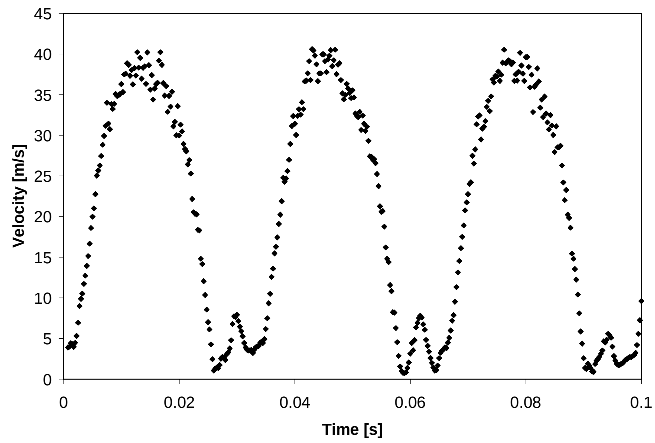

Figure 4 Typical inlet velocity profile

FLOW DISTRIBUTION MEASUREMENTS - The flow distribution was determined by measuring velocity profiles at the rear of the substrate. For the velocity measurements a TSI IFA 300 Constant Temperature Hot Wire Anemometry (HWA) system was used, as seen in figure 5. The system comprises of a main unit with the HWA bridges, a 2D traverse and the ThermalPro software to control and acquire data. The probes were 5 μm Tungsten/Platinum wires, calibrated using a TSI 1129 fully automatic calibration rig. The velocity profiles were measured in the outlet sleeve 30 mm downstream of the substrate. Previous work [9] showed that this distance was necessary in order to avoid jets from individual channels.

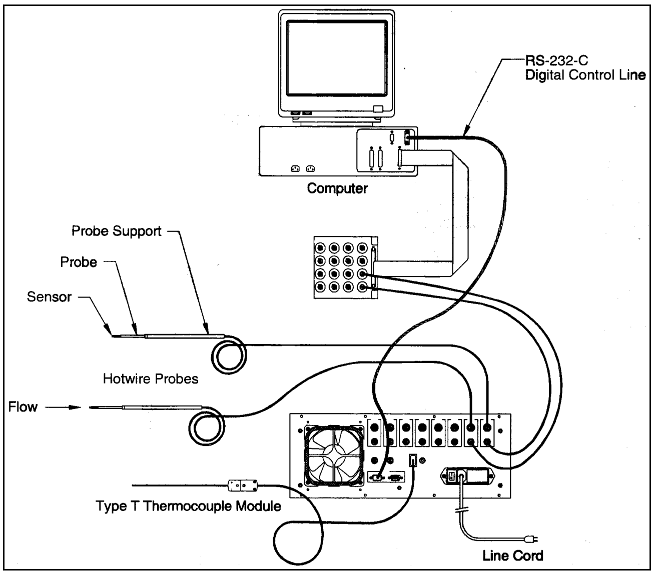

Figure 5   Overview of the IFA 300 System (Courtesy of TSI) [10]

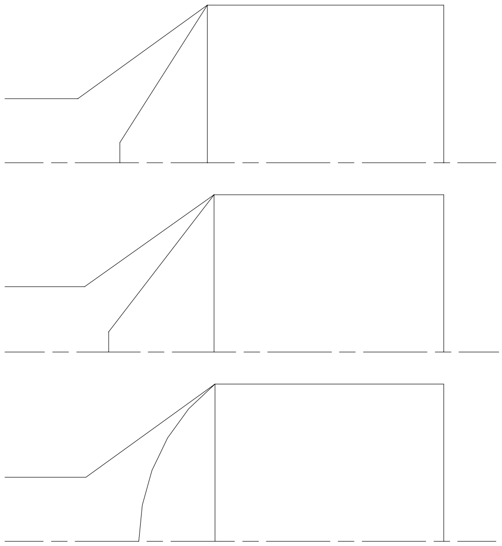

Figure 6   Schematics of substrates in baseline position

The flow distribution was measured along two perpendicular axes, X and Y for all four substrates. The inlet tube diameter that coincides with the plate edge when the duct hole is half open was defined as the x-axis (horizontally). The diameter at right angles to this was defined as the y-axis (vertically).

Initial experiments found distorted flow symmetry, especially at low frequencies along the Y-axis. This was found to be caused by pressure build-up behind the pulse generator. The problem was solved by locating 150 mm of flow straightener 40 mm downstream of the pulse generator. The flow straightener was made from 400 cpsi ceramic substrate and was divided into three 50 mm lengths separated by 20 mm gaps and finishing 20 mm up-steam of the diffuser throat.

Measurements were taken at four different flow rates, ranging from 20000 to 110000 and four different pulsation frequencies. The pulsation frequencies used were 16, 32, 64 and 100 Hz +/- 3 Hz. These flow rates and frequencies are representative of typical conditions found in firing engines. During all experiments the substrates were positioned in their base line position as seen in figure 6.

In this study because the substrate length varies radially space velocity was considered as the preferred measure of flow performance. Hence a non-uniformity index was devised to compare the performance of the substrates and was calculated using the mass flow weighted difference between the local and mean space velocity integrated over the substrate face. The local space velocity and the mean space velocity are defined as in equation 1 and 2 respectively.

$$V_{spi} = \frac{V_i}{L_i} \quad (1)$$

$$\bar{V}_{sp} = \frac{1}{\dot{m}} \int_A V_{spi} \delta \dot{m} \quad (2)$$

The variation of the space velocity, σ_{Vsp}, was defined according to equation 3.

$$\sigma_{Vsp} = \frac{1}{\dot{m}} \int_A \left| V_{spi} - \bar{V}_{sp} \right| \delta \dot{m} \quad (3)$$

This results in the non-uniformity index over the cross section of the substrate according to equation 4. A non-uniformity index of zero means that the space velocity is uniform across the substrate.

$$\psi = \frac{\sigma_{Vsp}}{\bar{V}_{sp}} \times 100 \quad (4)$$

EXPERIMENTAL RESULTS

The non-uniformity index plotted against Reynolds number can be seen in figures 7 to 10. The solid lines are second order polynomials fitted for improved visualisation. It is clear that the contoured substrates are less sensitive to changes in flow rate and pulsation frequency compared to the standard substrate and provided a much more uniform flow distribution.

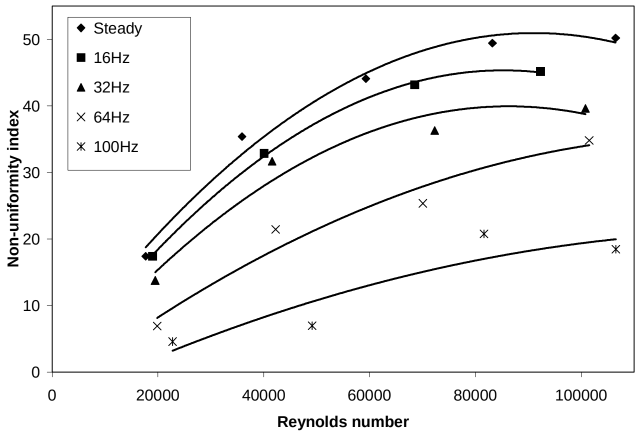

Figure 7 Non-uniformity against Reynolds number for the Standard substrate

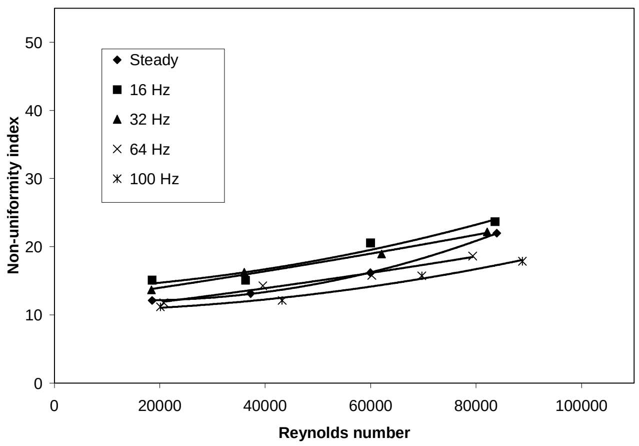

Figure 8 Non-uniformity against Reynolds number for the Contura 1 substrate

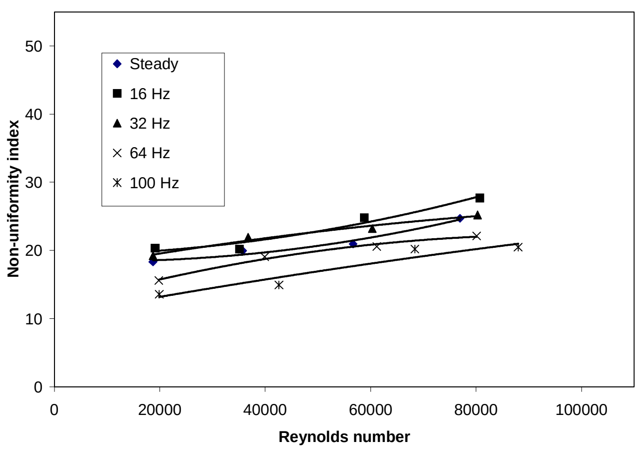

Figure 9 Non-uniformity against Reynolds number for the Contura 2 substrate

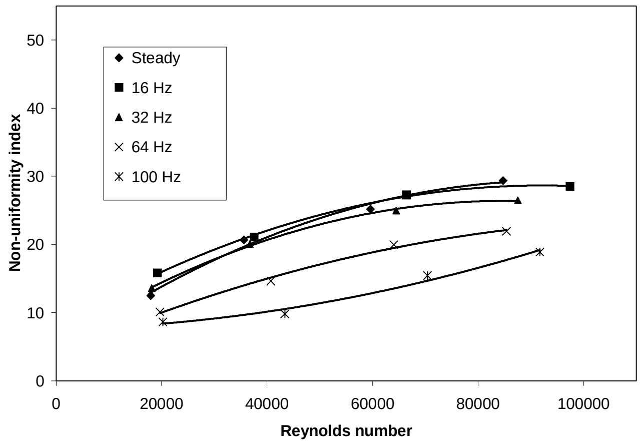

Figure 10 Non-uniformity against Reynolds number for the AeroCat substrate

The flow distribution measured at the rear of the substrates for the highest Re numbers is shown in figures 11 to 15. For the comparison non-dimensionalised space velocity was used, which is defined as local space velocity (eq. 1) divided by the mean space velocity (eq. 2). The non-dimensionalised space velocity was used to reduce any effects due to mass flow variations under which the experiments were undertaken.

Good flow symmetry was achieved for both steady and pulsating conditions, therefore for clarity only the non-dimensionalised space velocities along the x-axis have been plotted in the figures.

Figures 11 to 15 also show the effect of substrate shape for different pulsation frequencies starting with steady flow. The results of the Contura 1 and Contura 2 experiments were very similar with Contura 1 achieving a better flow uniformity. The Contura 2 results were therefore not presented in the figures.

The contoured substrates force the flow towards the outer radius producing a pronounced secondary maximum. This results in a lower non-uniformity index at all the frequencies.

Figures 16 to 18 show the effect of different frequencies for the Standard substrate, Contura 1 and AeroCat substrates. It can be seen that the flow distributions at 16 and 32 Hz were similar to the steady state cases. However as the frequency reaches 64 and 100 Hz significantly more uniform velocity profiles can be seen for all substrates.

These beneficial effects were believed by Zhao *et al.* [11] to be caused by pulsations acting similarly to large-scale turbulence, enhancing mixing.

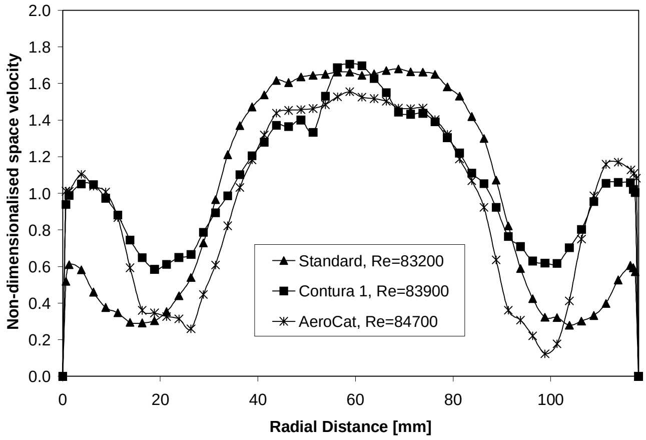

Figure 11 Non-dimensionalised space velocity profiles along the x-axis for the Standard, Contura 1 and AeroCat substrate at steady flow

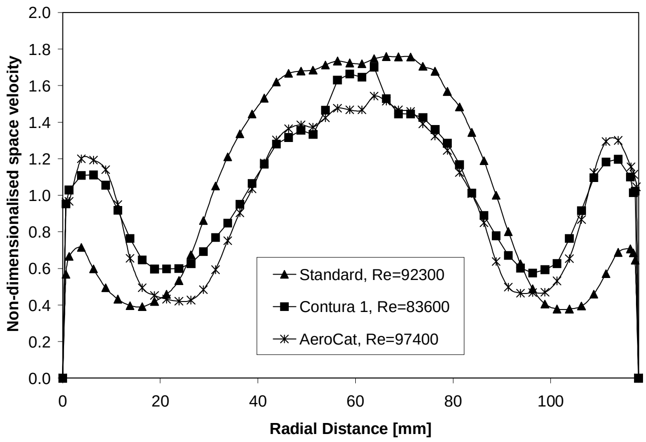

Figure 12 Non-dimensionalised space velocity profiles along the x-axis for the Standard, Contura 1 and AeroCat substrate at 16 Hz

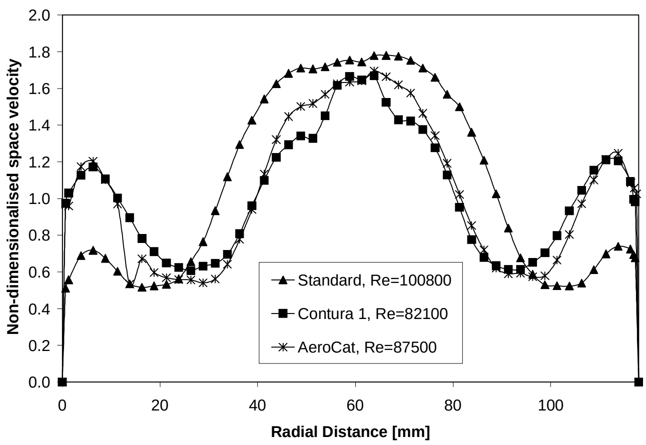

Figure 13 Non-dimensionalised space velocity profiles along the x-axis for the Standard, Contura 1 and AeroCat substrate at 32 Hz

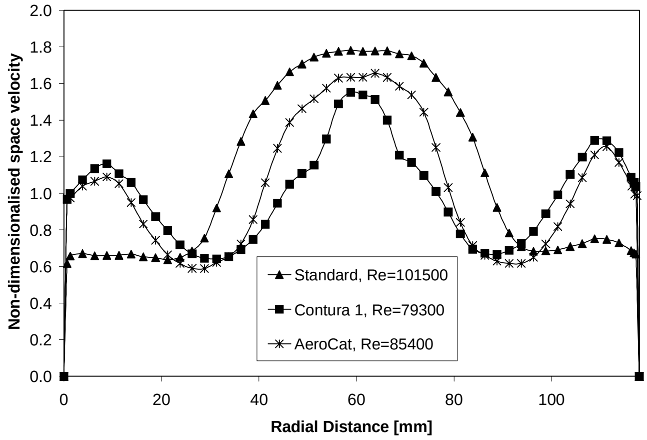

Figure 14 Non-dimensionalised space velocity profiles along the x-axis for the Standard, Contura 1 and AeroCat substrate at 64 Hz

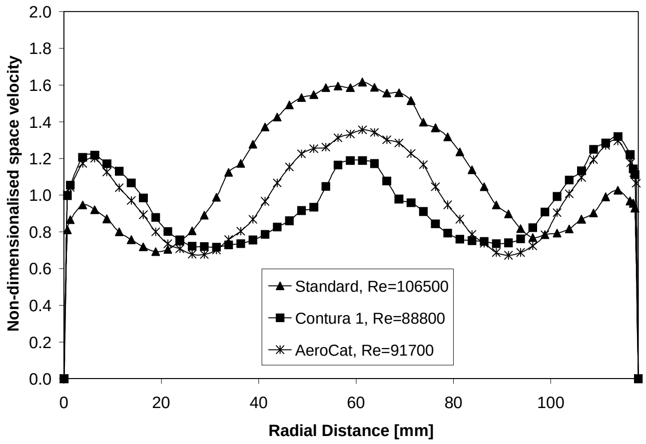

Figure 15 Non-dimensionalised space velocity profiles along the x-axis for the Standard, Contura 1 and AeroCat substrate at 100 Hz

Figures 19 to 21 compare space velocity profiles for a constant pulsation frequency of 100 Hz for different Re numbers. It can be seen that the flow maldistribution increases with increased flow rate even under pulsating conditions. The rate of increase was however found to be lower for the contoured substrates when compared to the standard substrate. This is believed to be due to the decreased diffuser volume, which helps to suppress flow separation in the diffuser throat at the higher Re numbers.

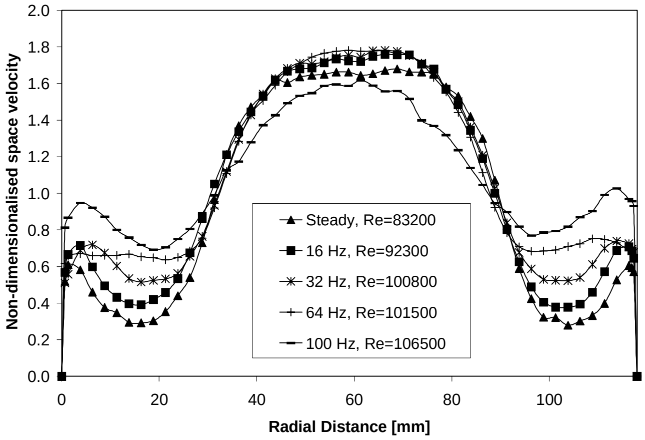

Figure 16 Non-dimensionalised space velocity profiles along the x-axis for the Standard substrate for a range of frequencies

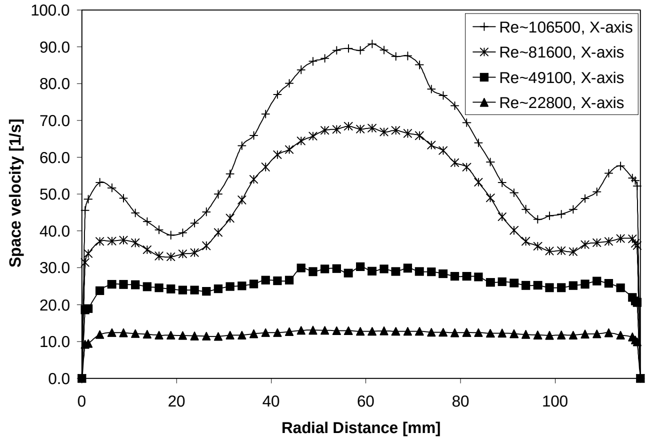

Figure 19 Space velocity profiles along the x-axis for the Standard substrate at a pulsation frequency of 100 Hz

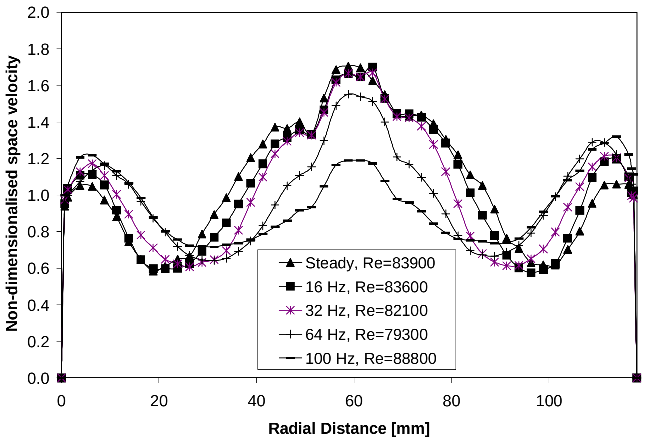

Figure 17 Non-dimensionalised space velocity profiles along the x-axis for the Contura 1 substrate for a range of frequencies

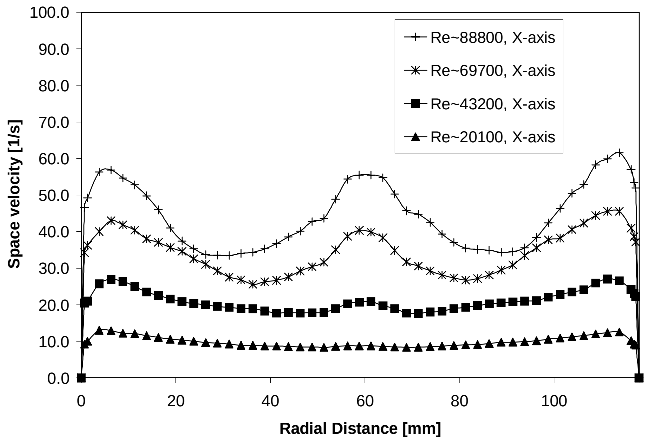

Figure 20 Space velocity profiles along the x-axis for the Contura 1 substrate at a pulsation frequency of 100 Hz

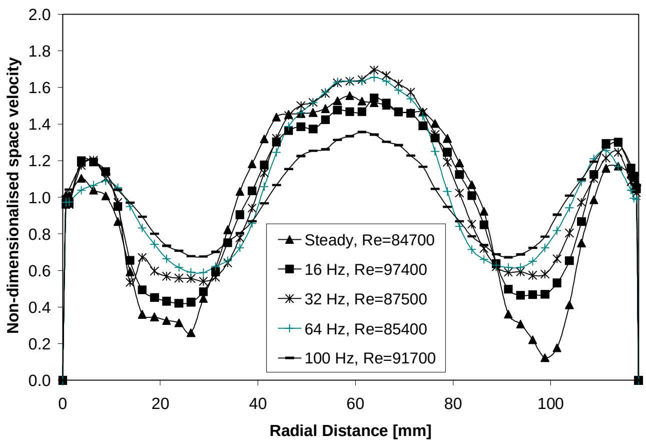

Figure 18 Non-dimensionalised space velocity profiles along the x-axis for the AeroCat substrate for a range of frequencies

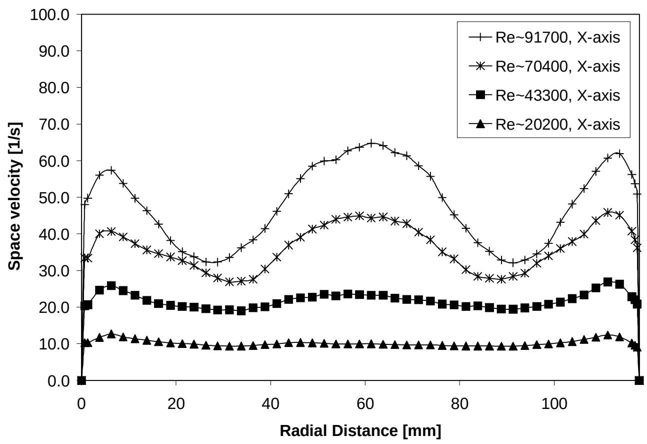

Figure 21 Space velocity profiles along the x-axis for the AeroCat substrate at a pulsation frequency of 100 Hz

CFD PREDICTIONS

In a previous paper [3] the authors presented results of CFD predictions for the standard and Contura 1 substrates. Although qualitative agreement with measurements was obtained the predictions produced flow profiles which where much too flat. The main problem was believed to be associated with entrance effects where the flow impinges obliquely on the front face of the substrate [9]. A method to account for such effects for standard substrates is described in [12, 13]. The approach is suggested by the early work on heat exchangers by Küchemann and Weber [14]. They suggested that an estimate of the extra pressure loss term may be given by equation 5 where u is the radial velocity component just up-stream of the substrate.

$$\frac{1}{2}\rho u^2 \qquad 5$$

This has been applied to the standard and Contura 1 substrates. CFD predictions were performed using the commercially available software package Star-CD. To simulate the substrate, a porous medium approach was used with the pressure drop prescribed using the Hagen –Poiseuille equation appropriate for square channels [9] plus the additional pressure loss term as given in equation 5. The non-linear k-ε turbulence model was used in the high Reynolds number regions and the Norris Reynolds model in the near wall region. All variables were discretised using a second order differencing scheme. The flow was assumed to be iso-thermal, incompressible and axially symmetric. Hence only a 5-degree wedge was simulated with symmetry planes defined at the wedge faces. The experimental results compared to CFD predictions for the Standard and Contura 1 substrate can be seen in figures 22 and 23.

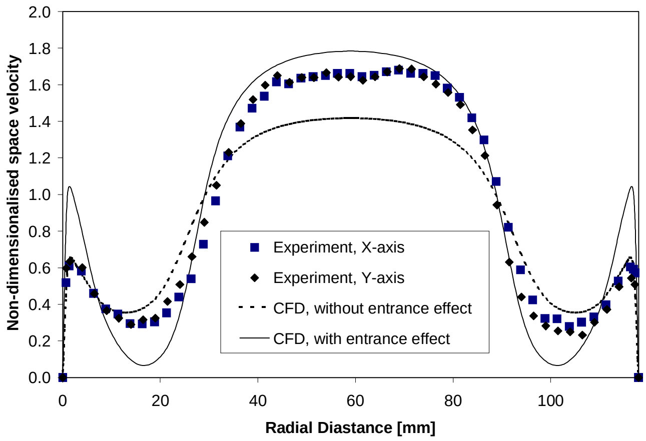

Figure 22 Experimental velocity profiles for the Standard substrate compared to CFD predictions with and without entrance effect, Re=83200.

Incorporating the entrance effect improves predictions especially within the important central region where high heat flux leading to rapid light-off occurs. Further improvements are clearly necessary and these are the subject of on-going research.

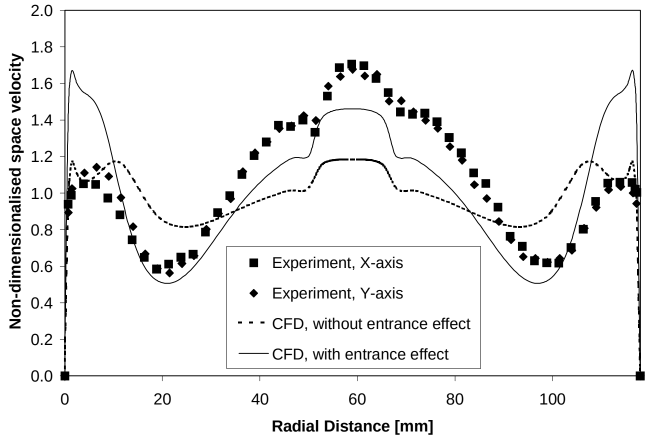

Figure 23 Experimental velocity profiles for the Contura 1 substrate compared to CFD predictions with and without entrance effect, Re=83900.

CONCLUSION

An investigation of the flow performance of ceramic contoured substrates under steady and pulsating conditions has been undertaken. It has been shown that the flow distribution can be improved by using shaped substrates.

It was also found that the flow uniformity for shaped substrates was less sensitive to changes in mass flow rate and pulsation frequency.

For the standard substrate the flow distribution was improved as pulsation frequency increased. For the contoured substrates it was found that the flow distribution at pulsation frequencies of 16 and 32 Hz was similar to the steady state cases. However at the higher frequencies of 64 and 100 Hz the flow distribution was found to be more uniform.

Improved CFD predictions were obtained when entrance effects were included, especially within the central region of the substrates.

ACKNOWLEDGMENTS

We would like to thank Corning Inc. for supplying the substrates. We would also like to thank David Lloyd-Thomas at Ford Motor Co., Analytical Powertrain, UK, for valuable discussions. We also acknowledge support under the SERC-DTI ACCP LINK scheme.

CONTACT

Dr S. F. Benjamin
Coventry University, School of Engineering
Priory Street, Coventry, CV1 5FB, United Kingdom
s.benjamin@coventry.ac.uk

REFERENCES

1. Howitt, J. S., Sekella, T. C., - *Flow effects in Monolithic Honeycomb Automotive Catalytic Converters*, SAE paper 740244, 1974.

2. Comfort, E. H., - *Monolithic Catalytic Converters Performance as a function of Flow Distribution*, ASME Winter Annual Meeting, Paper No. 74-WA/HT-30, 1974.

3. Wollin, J., Benjamin, S. F., - "*A Study of the Flow Performance of Ceramic Contoured Substrates for Automotive Exhaust Catalyst Systems*", 1999 SAE Transactions, Vol. 108, Journal of Fuels & Lubricants, Section 4, pages 2014-2021.

4. Heibel, A., and Spaid, M. A. A., - *A New Converter Concept Providing Improved Flow Distribution and Space Utilization*, Corning Inc. SAE Spring Fuels and Lubricants, SAE 990768, 1999.

5. Schönfelder, C., - *Strömungsoptimierung von metallishen Automobil-Abgaskatalysatoren*, *VDI Berichte*, 613, pp 801-818, 1986.

6. Holmgren, A., Grönstedt, T., Andersson, B., - *Improved Flow Distribution in Automotive Monolithic Converters*, Chalmers University of Technology, Gothenburg, Sweden, 1997.

7. Shuai, S., Wang, J., Zhuang, R., Chen, J., - *The Effects of Structure of Automotive Catalytic Converters on its Flow Distribution*, Chinese Automotive Engineering, vol. 22, no. 1, 2000.

8. Shuai, S., Wang, J., Zhuang, R., Chen, J., - *Study on Flow Characteristics of Automotive Catalytic Converters with Various Configurations*, SAE Int. Conference, USA, SAE 2000-01-0208, 2000.

9. Benjamin S. F., Clarkson R. J., Haimad N. and Girgis N. S. - *An experimental and predictive study of the flow in axisymmetric automotive exhaust catalyst systems,* 1996 SAE Transactions, Vol. 105, Journal of Fuels and Lubricants, Section 4, pages 1008-1019.

10. TSI Inc. Fluid Mechanics Instrument Division, - *IFA Constant Temperature Anemometer System, Instruction Manual,* Part no 1990746, May 1997.

11. Zhao, F.-Q., Li, L., Xie, X., Lai, M.-C. – *An Experimental Study of the Flow Structure Inside the Catalytic Converter of a Gasoline Engine*, SAE Int. Conference, Detroit, USA, SAE 950784, 1995

12. Haimad, N., - *A Theoretical and Experimental Investigation of the Flow Performance of Automotive Catalytic Converters*, PhD thesis, Coventry University, 1997.

13. Benjamin, S. F., Haimad, N., Roberts, C. A., Wollin, J., - *Modelling the Flow Distribution through Automotive Catalytic Converters*, Submitted to Proc. Inst. Mech. Engs., Part C, Journal of Mechanical Engineering Science, 2000.

14. Küchemann, D., Weber, J., - *Aerodynamics of Propulsion*, McGraw-Hill Book Co. Inc. 1953.

NOMENCLATURE

A	Cross sectional area [m^2]
d	Diameter of inlet pipe [m]
L_i	Local channel length [m]
$\dot{m}$	Mass flow rate [kg/s]
Re	Reynolds number in inlet pipe
U_{in}	Mean velocity in the inlet pipe [m/s]
V_i	Local velocity [m/s]
V_{spi}	Local space velocity [1/s]
V_{sp}	Mean space velocity [1/s]
μ	Dynamic viscosity [kg/m s]
ρ	Air density from ideal gas law [kg/m^3]
ψ	Non-uniformity index
σ_{Vsp}	Variance of non-uniformity [1/s]

Reynolds No. $$\mathrm{Re} = \frac{\rho \times U_{in} \times d}{\mu}$$